Electronic Supplementary Material (ESI) for Analyst.
This journal is © The Royal Society of Chemistry 2023

Supporting Information

Intramolecular aptamer switches

Lu Shi [a,b], Yan Jin [a]*, and Juewen Liu [b]*

[a] Key Laboratory of Analytical Chemistry for Life Science of Shaanxi Province, Key Laboratory of Applied Surface and Colloid Chemistry, Ministry of Education, School of Chemistry and Chemical Engineering, Shaanxi Normal University, Xi'an 710119, China

[b] Department of Chemistry, Waterloo Institute for Nanotechnology, University of Waterloo, Waterloo, ON N2L 3G1, Canada

* Correspondence:

liujw@uwaterloo.ca (Juewen Liu);

jinyan@snnu.edu.cn (Yan Jin)

Table of Content

Table S1. Sequences of the oligonucleotides used in the experiments. The nucleotides in boldface are added to form the initial state of the switches.

Names	Sequences (5'-3')
OTC5	ACGACATTCCGTTGATCTCTCCCTTTTGGGTTGGTGTCGT
OTC5-7bp	**ACCA**ACCACATTCCGTTGATCTCTCCCTTTTGGGTTGGTGTGGT
OTC5-8bp	**CACCA**ACCACATTCCGTTGATCTCTCCCTTTTGGGTTGGTGTGGT
OTC5-9bp	**ACACCA**ACCACATTCCGTTGATCTCTCCCTTTTGGGTTGGTGTGGT
OTC5-10bp	**CACACCA**ACCACATTCCGTTGATCTCTCCCTTTTGGGTTGGTGTGGT
cDNA-OTC5-8bp	CACCAACC
Es2	CGACTTAAGGTATGTGATCTTAGTTGTAGTTCAAGTCG
Es2-7bp	GGACTTAAGGTATGTGATCTTAGTTGTAGTTCAAGTCC**TTAAG**
Es2-8bp	GGACTTAAGGTATGTGATCTTAGTTGTAG TTCAAGTCC**TTAAGT**
Es2-9bp	GGACTTAAGGTATGTGATCTTAGTTGTAGTTCAAGTCC**TTAAGTC**
Es2-10bp	GGACTTAAGGTATGTGATCTTAGTTGTAG TTCAAGTCC**TTAAGTCC**
Ade1304b	ACGACACGGAGGCTTAGTTTGCTAAATGGTCATGTCGT
Ade1304b-7bp	**AGCAA**ACGACACGGAGGCTTAGTTTGCTAAATGGTCATGTCGT
Ade1304b-8bp	**TAGCAA**ACGACACGGAGGCTTAGTTTGCTAAATGGTCATGTCGT
Ade1304b-9bp	**TTAGCAA**ACGACACGGAGGCTTAGTTTGCTAAATGGTCATGTCGT
Ade1304b-10bp	**TTTAGCAA**ACGACACGGAGGCTTAGTTTGCTAAATGGTCATGTCGT

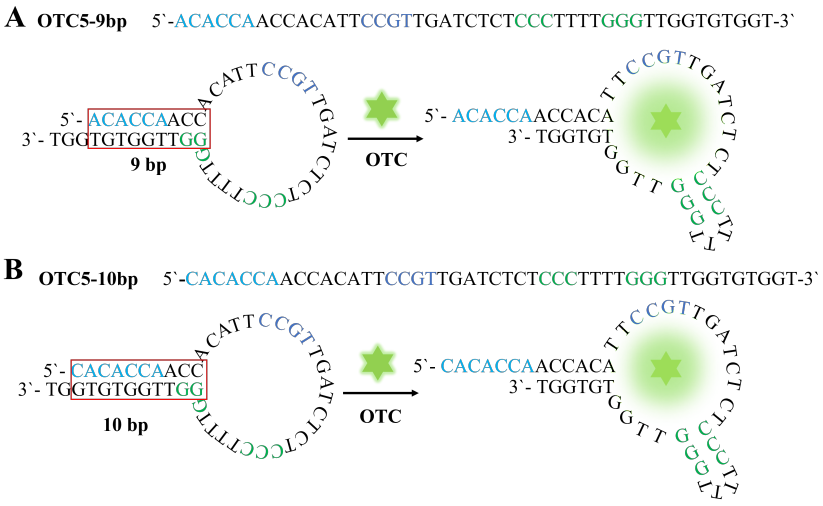

Figure S1. (A) The design of sequence of OTC5-9bp and schematic illustration of intramolecular conformational change upon target binding. (B) The design of sequence of OTC5-10bp and schematic illustration of intramolecular conformational change upon target binding. The intrinsic fluorescence of OTC is enhanced by binding to the aptamer.

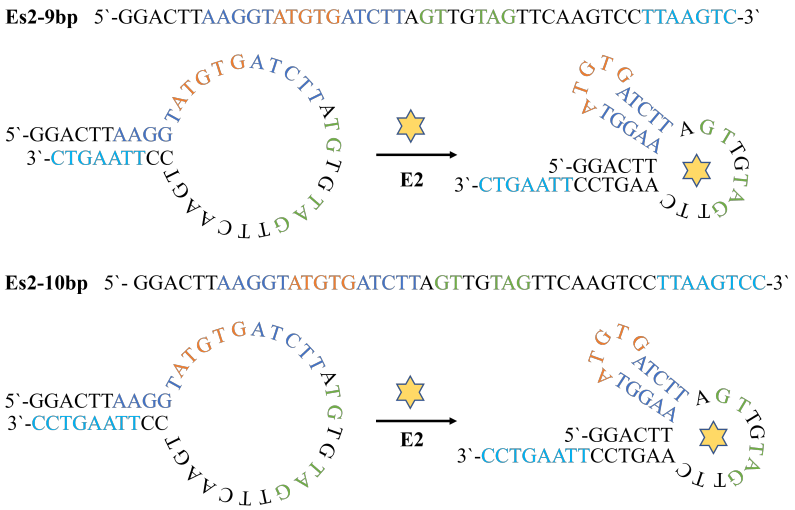

Figure S2. (A) The design of sequence of Es2-9bp and schematic illustration of intramolecular conformational change upon target binding. (B) The design of sequence of Es2-10bp and schematic illustration of intramolecular conformational change upon target binding.

To achieve an optimal detection performance, we optimized various parameters, such as SGI concentration, and the concentrations of Mg^{2+} and Na^{+} in the buffer. In Figure S3A, there is a noticeable increase in fluorescence intensity as the concentration of SGI was increased. To determine the optimal concentration of SGI, we evaluated the ratio F/F_0, where F is the fluorescence signal in the presence of E2, and F_0 is the signal without E2. Figure S3B reveals that the F/F_0 ratio diminishes as the SGI concentration rises. To achieve a superior F/F_0 and F value, we selected 0.1× SGI for further studies. Figures S3C and D reveal that variations in Na^{+} concentration result in only minor changes to the fluorescence signal. It suggests that Na^{+} minimally influences the recognition reaction between E2 and aptamer. A similar observation is held for Mg^{2+} (Figures S3E and F). Consequently, we selected 100 mM NaCl and 8 mM $MgCl_2$ for further studies.

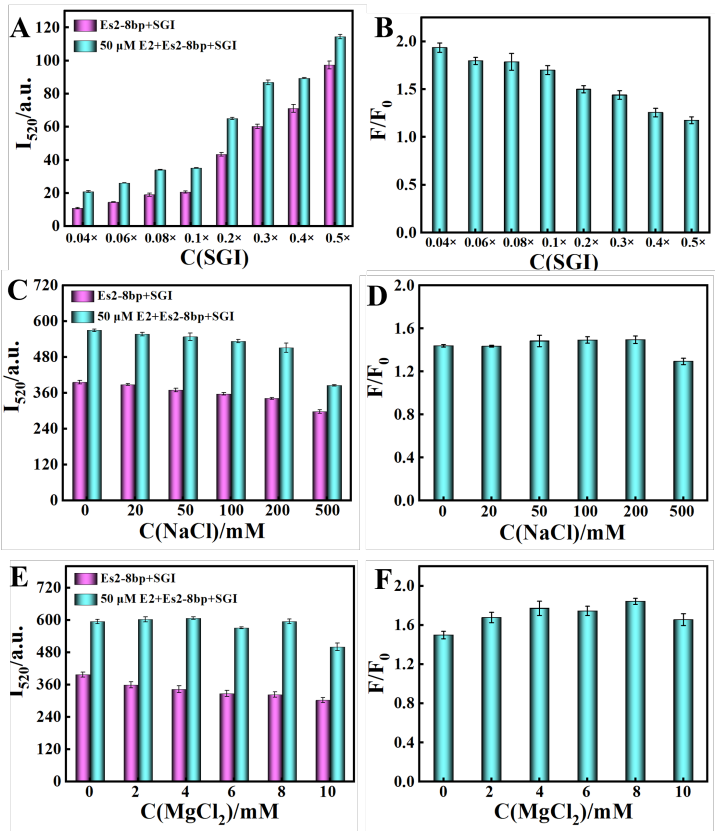

Figure S3. Fluorescence intensity and change (F/F_0) of SGI/Es2-8bp in the presence of different concentrations of (A, B) SGI, (C, D) NaCl and (E, F) $MgCl_2$. The concentrations of the aptamers and SGI were 200 nM and 0.1×, respectively. The error bars represented the standard deviation of three independent measurements.

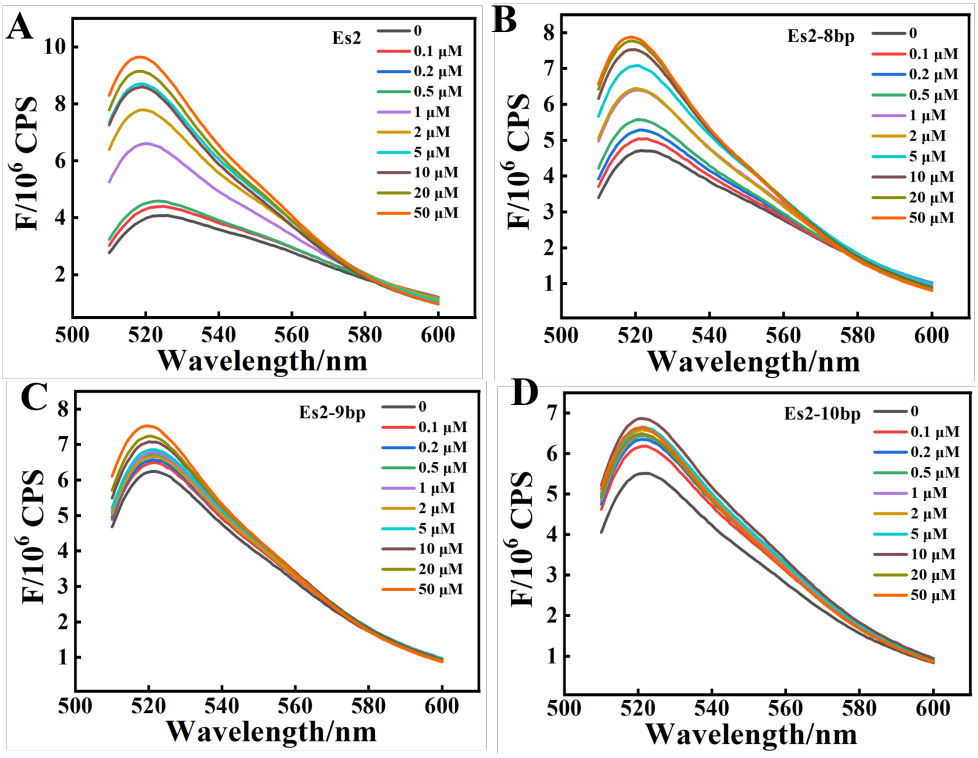

Figure S4. Fluorescence spectra of SGI/Es2 (A), SGI/Es2-8bp (B), SGI/Es2-9bp (C), SGI/Es2-10bp (D) in the presence of different concentrations of E2. The concentration of aptamer and SGI were 200 nM and 0.1×, respectively.

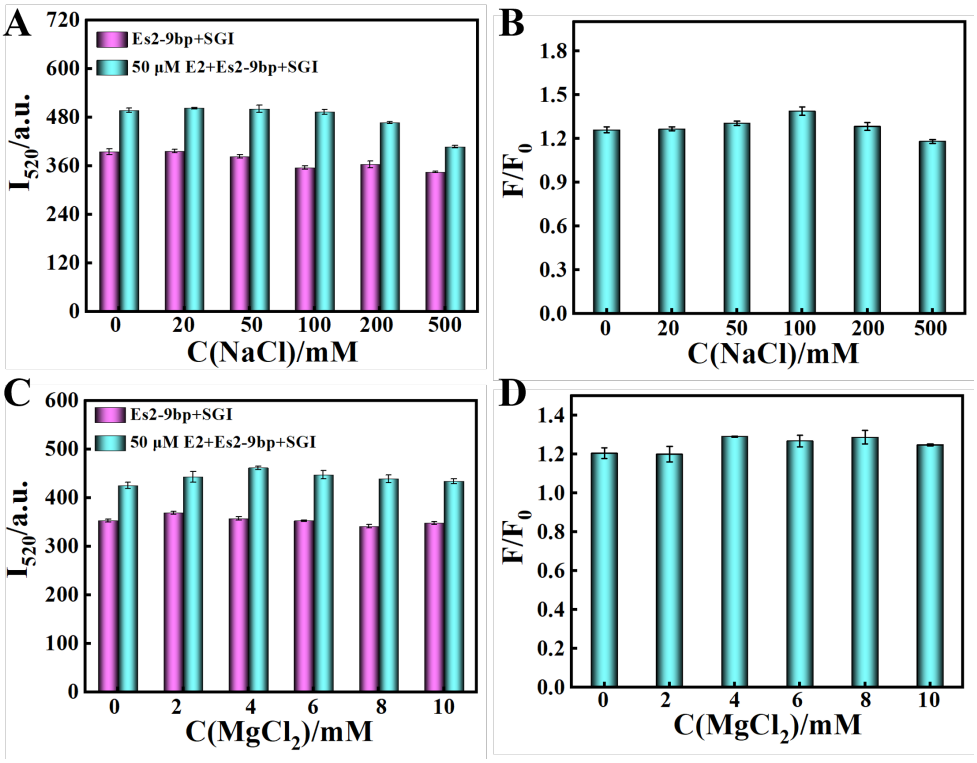

Figure S5. Fluorescence intensity and change (F/F_0) of SGI/Es2-9bp in the presence of different concentrations of NaCl (A, B) and $MgCl_2$ (C, D). The concentrations of the aptamers and SGI were 200 nM and 0. ×, respectively. The error bars represented the standard deviation of three independent measurements.

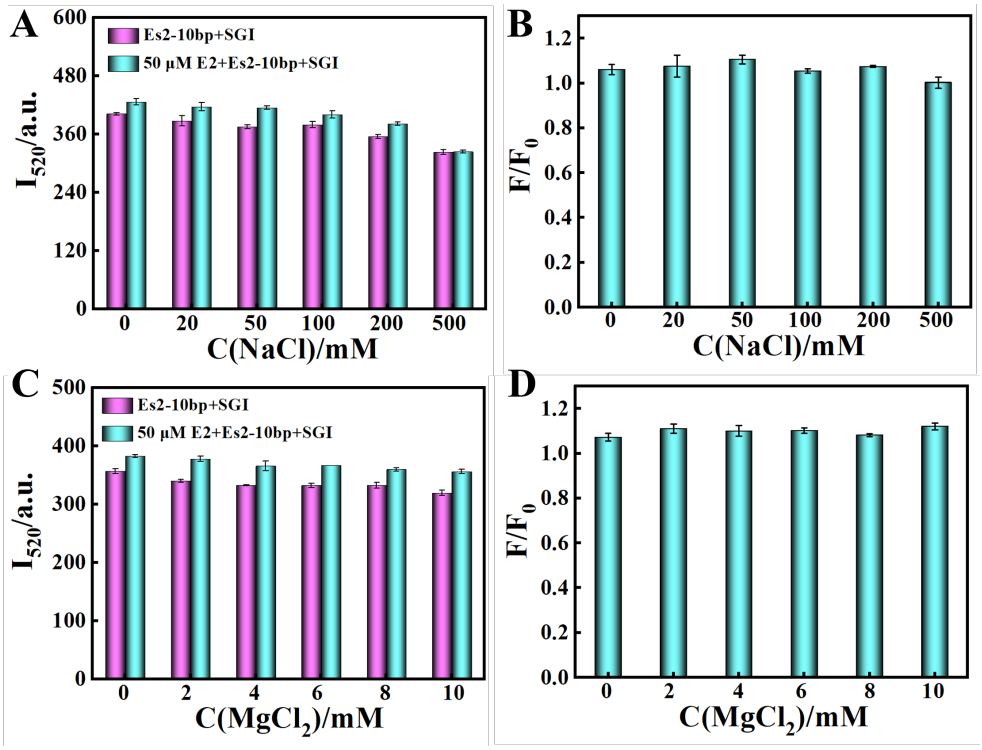

Figure S6. Fluorescence intensity and change (F/F_0) of SGI/Es2-10bp in the presence of different concentrations of NaCl (A, B) and $MgCl_2$ (C, D). The concentrations of aptamer and SGI were 200 nM and 0.1×, respectively. The error bars represented the standard deviation of three independent measurements.

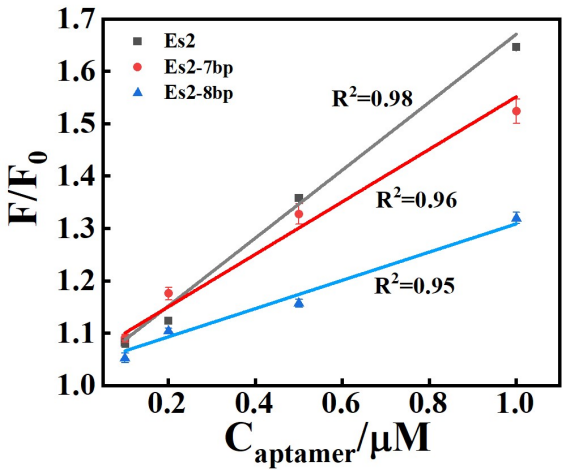

Figure S7. Plots of F/F_0 as a function of E2 concentrations. The concentration of aptamer and SGI were 200 nM and 0.1×, respectively. The error bars represented the standard deviation of three independent measurements.

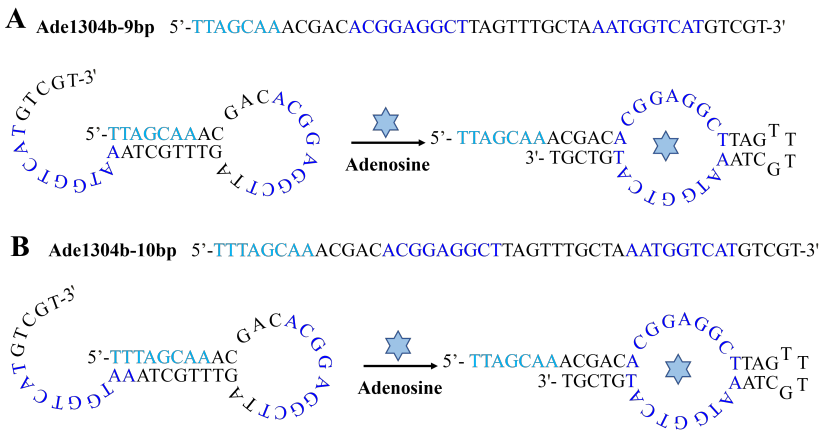

Figure S8. (A) The design of sequence of Ade1304b-9bp and schematic illustration of intramolecular conformational change upon target binding. (B) The design of sequence of Ade1304b-10bp and schematic illustration of intramolecular conformational change upon target binding.

As illustrated in Figure S9A, the fluorescence of ThT/apt is notably lower in the presence of the target compared to its absence. As the ThT concentration gradually increases, so does the fluorescence intensity. Simultaneously, the F/F_0 shows an increasing trend with rising ThT concentration (Figure S9B). Considering the "turn-off" nature of the sensor and the potential impact of excessively low ThT concentrations on assay sensitivity and reproducibility, 2 μM ThT was selected for further research.

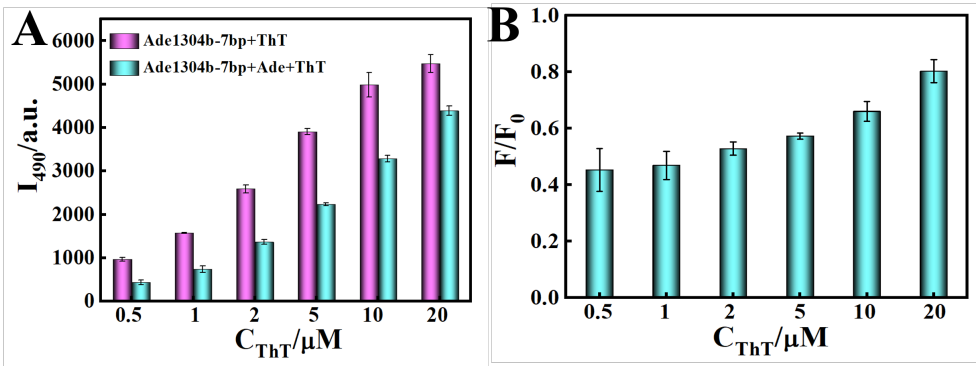

Figure S9. Fluorescence intensity and change (F/F_0) of ThT/Ade1304b-7bp in the presence of different concentrations of ThT. The concentrations of the aptamer was 100 nM. The error bars represented the standard deviation of three independent measurements.

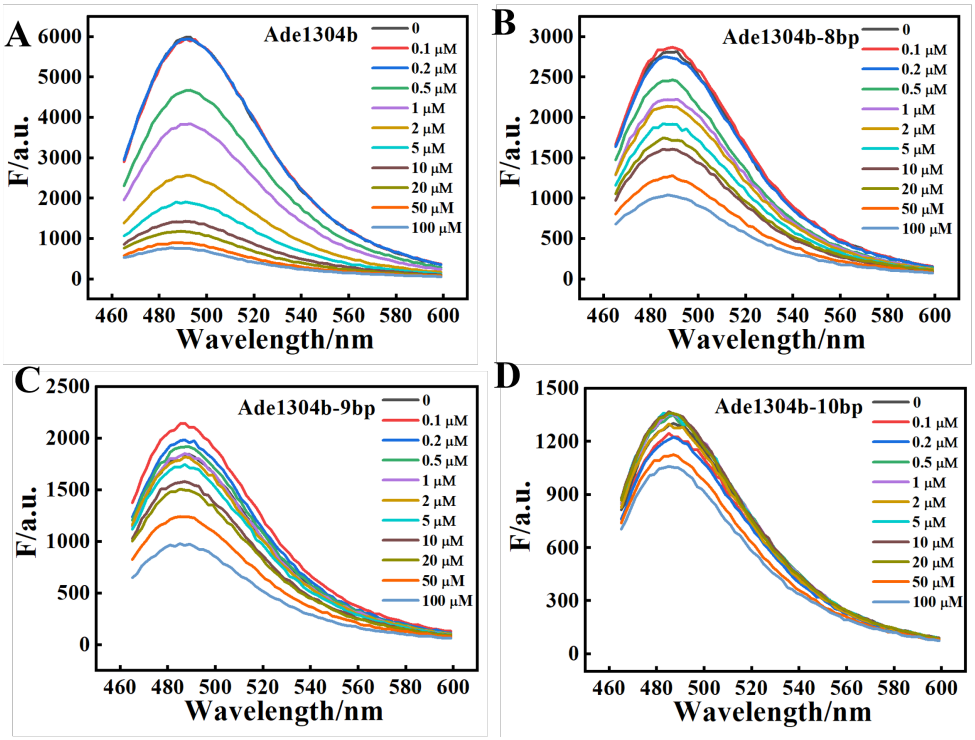

Figure S10. Fluorescence spectra of ThT/Ade1304b (A), ThT/Ade1304b-8bp (B), ThT/Ade1304b-9bp (C), and ThT/Ade1304b-10bp (D) in the presence of different concentrations of adenosine. The concentrations of the aptamers and ThT were 100 nM and 2 μM, respectively.